SEAGULL: Low-Cost Pervasive Sensing for Monitoring and Analysing Underwater Plastics

Huber Flores[1], Agustin Zuniga[2], Marko Radeta[3], Zhigang Yin[1], Mohan Liyanage[1], Naser Hossein Motlagh[2], Ngoc Thi Nguyen[2], Sasu Tarkoma[2], Moustafa Youssef[4], Petteri Nurmi[2]
[1]University of Tartu, Estonia;[2]University of Helsinki, Finland;
[3]Wave Labs, MARE/ARNET/ARDITI, University of Madeira, Portugal; University of Belgrade, Serbia;
[4]The American University in Cairo, Egypt
{firstname.lastname@}ut.ee, helsinki.fi, wave-labs.org

***Abstract*—We contribute SEAGULL, a novel pervasive sensing approach for monitoring and identifying underwater plastics. SEAGULL builds on an innovative light (LED) sensing solution that takes advantage of convolutional sparse coding to classify plastic debris according to their material (resin identification code). This enables SEAGULL to determine the composition of plastics in-situ, unlike existing plastic analysis methods which require taking the samples to a laboratory where they are analyzed using high precision measurement instruments. Through extensive experiments we demonstrate that SEAGULL correctly distinguishes between the main plastic categories (over 85% accuracy), is able to operate robustly against diverse water conditions (turbulence, turbidity, luminosity), and works with different sensing resolutions. We also demonstrate the practicality of SEAGULL by carrying out field tests in an ocean and a river, demonstrating that the performance of SEAGULL translates to real in-the-wild environments. Our work demonstrates how low-cost pervasive sensing solutions help to tackle environmental sustainability challenges, offering a new way to collect information about the extent and characteristics of underwater plastics and improving the scale at which monitoring can operate while overcoming the main constraints of existing techniques.**

***Index Terms*—Marine pollution, Aquatic debris, Light sensing, Pervasive Sensing, Internet of Things, Underwater sensing.**

I. Introduction

Plastic pollution is a growing worldwide concern and a leading environmental sustainability challenge. Plastic pollutants have many adverse effects affecting everything from the health of marine ecosystems to weather patterns and even human health [1]. While there has been a concentrated effort to reduce the use of plastics, e.g., through bans of single-use plastics [2], the situation remains highly delicate. Indeed, as certain plastic types have decreased, others have increased. For example, increased use of personal protective equipment during the COVID-19 pandemic surged plastic pollution in oceans [3]. Improving the situation requires accurate information about both the density and the characteristics of plastics. Indeed, knowing the *type* of plastic is important for guiding cleaning efforts, understanding and modeling the effects of the plastics on local and global ecosystems, and identifying the root cause of the plastics. The type of plastic also affects the degradation process, including the toxicity of the plastics and the potential chemicals they may release, which are essential to know to guide cleaning efforts [4]. Hence, obtaining information about their materials is vital for determining the best possible countermeasure. Having effective plastic monitoring is also a legal requirement for national environmental agencies and having mechanisms to support this process can significantly improve the resolution of information that is being collected.

Obtaining accurate information about the extent and characteristics of pollutants is challenging as current approaches are limited to approximating the total extent of pollutants without providing details of their composition or rely on time-consuming and laborious processes that have significant delay between data collection and analysis. The extent of pollutants is typically estimated from water samples using microscopy [5] but this only captures the total amount of plastic particles without offering insights into what caused them or how to reduce pollution. The type of pollutants is typically monitored using laboratory analysis and (visual) surveying. These methods first collect a sample using, bottom trawls, beach surveys of stranded plastics, towing or diving surveys, aerial imaging or related techniques [6]–[9]. The samples are then taken to a laboratory where they are cleaned, prepared, and analysed using high-precision measurement tools, e.g., based on infrared spectroscopy [10]. This process is highly laborious and time-consuming, resulting in significant delay between data collection and analysis. The methods used to collect samples also have significant limitations, e.g., bottom trawls damage the marine ecosystem, whereas beach, towing, and diving surveys have small spatial and temporal scale. Finally, aerial surveys are restricted to plastics that float, covering only approximately 5% of all plastics [11]. While there have been some efforts to develop technologies to support plastic monitoring, e.g., using underwater video captured from drones or static camera deployments [12]–[15] or aerial footage [16], [17], these merely automate some aspects of the monitoring process without overcoming other limitations. For example, vision-based methods can only identify debris without being able to identify the composition of plastics, and their performance is affected by water conditions [18], [19]. These solutions also suffer from long delays as the footage is typically collected during other activities and analyzed on the surface where sufficient computational power is available [20]. Obtaining accurate, timely, and actionable information about the extent and composition of plastics requires novel solutions that can mitigate these limitations of current techniques.

We contribute SEAGULL as a novel low-cost pervasive

979-8-3503-7025-6/24/$31.00 ©2024 IEEE
DOI 10.1109/IoTDI61053.2024.00009

sensing solution that detects and classifies underwater plastics. SEAGULL can be integrated with existing underwater data collection practices (scuba divers or ROVs) and can analyze in-situ without requiring taking the samples to a laboratory for detailed analysis. SEAGULL achieves this using an innovative optical sensing approach that uses inexpensive and off-the-shelf components (LEDs and photo-receptors) and convolutional sparse coding to identify debris and determine the material of the object according to the resin identification code (RIC). Ensuring the sensing pipeline can operate accurately and robustly is highly challenging as we need to overcome challenges caused by varying underwater conditions. Specifically, light intensity measurements are affected by noise and changes in the ambient environment. At the same time, the power draw of the sensing pipeline should be sufficiently small to support long-term operation. SEAGULL addresses noise in the light reflectance measurements by taking advantage of an innovative convolutional sparse coding technique that breaks the overall light spectrum into latent components that correspond to smaller constituents of the overall spectrum. As we demonstrate, these latent components are more resilient to noise, significantly improving the accuracy and robustness of SEAGULL. We also demonstrate the further improvements can be achieved by integrating additional sensor modalities with SEAGULL, e.g., accelerometers and gyroscopes can be used to detect periods that have better quality signals.

Through extensive experiments we demonstrate that SEAGULL correctly distinguishes between the main plastic categories (over 85% accuracy), operates robustly under different water conditions (turbulence, turbidity, luminosity), and works with different sensing resolutions. We also demonstrate that SEAGULL can identify plastic debris more precisely than a computer vision-based object detector baseline. SEAGULL can complement and enrich existing methods by collecting more details about the composition and characteristics of pollutants without requiring retrieval of the plastic debris for subsequently laboratory analysis. Finally, we demonstrate the practicality of SEAGULL by carrying out field tests in a sea (with scuba divers) and a river (ROV). The results of these tests demonstrate that our results also translate to differing real-world underwater environments. Taken together, SEAGULL offers an innovative solution for tackling underwater plastics, an important environmental sustainability challenge, that is low-cost yet effective and capable of operating across different underwater conditions.

II. Plastics in Aquatic Ecosystems

Plastics are identifiable from their *resin identification code* (RIC) which refers to the type of resin that is used in the manufacturing process. The most common plastics used in everyday products belong to six RIC categories; see Table I. The RIC type affects the manufacturing process, but also the characteristics of the resulting plastic in aquatic environment. For example, PET sinks in water due to its higher density than water whereas LDPE, HDPE and PP remain afloat due to their lower density [21].

TABLE I: Plastic samples considered in the experiments along with their family properties. RIC: Resin Identification Code.

RIC	Acron.	Uses
01 PET	PET	soft drinks plastic bottles, polyester yarn and fibers, clamshell packaging
02 PE-HD	HDPE	disposable suits, shampoo bottles shopping bags, playground equipment, food storage containers
03 PVC	PVC	vinyl gloves, plastic cards (bank, ids, loyalty), pipes, inflatable products
04 PE-LD	LDPE	six pack rings, laminated juice and milk cartons, plastic wraps, trays
05 PP	PP	respiratory masks filters, sanitary products, diapers, yarns and textiles,suture prolene
06 PS	PS	foodservice packaging, instrument panels, thermal insulation in walls and roofs

Knowing the exact *type* of plastics is essential for several reasons. First, besides differing in density, plastics differ in terms of toxicity and the manufacturing processes use differing chemicals which also affect the environmental effects of the plastics [22]. Knowing the type of plastics thus helps to determine the most effective cleaning methods, as well as helps to identify potential chemicals that may have leaked to the environment. Second, knowing the type of plastic can help identify the source of plastics. PET mostly results from bottles that have been transported by weather or animals from landfills and beaches, PS mostly results from plastic pellets, and HDPE mostly originates from fishing nets [23]. Third, plastics differ in their degradation process which determines how fast they break into smaller fragments that are then ingested by aquatic animals [24]. Taken together, knowing the exact type of plastic is essential for mitigating the adverse effects of aquatic plastics and for designing effective countermeasures to address them.

III. Motivating Example with Computer Vision

Plastic pollutants are commonly monitored using manual data collection techniques, such as visual counting and tagging debris with GPS. While these approaches can detect the presence of plastics, they cannot identify the type of plastic, which is essential for guiding effective cleaning and modeling the broader effects on local and global ecosystems. The main automated (or semi-automated) monitoring solution is to rely on computer vision which can operate as part of statically deployed cameras (e.g., buoys or moorings) [12]–[14] or be carried by divers or integrated in ROVs as they survey the oceans [15], [25]. We next demonstrate that computer vision is only sufficient for detecting plastic debris, but not for characterising the composition of the plastic objects.

We run small-scale experiments using a state-of-the-art deep learning object detection architecture (MobileNet V2 [26]) using Single Shot MultiBox Detector (SSD). The process for training, validation and inference is the same as described by Fulton et al. [12]. We rely on this model as it has been shown to achieve good performance in trash detection [12] and is

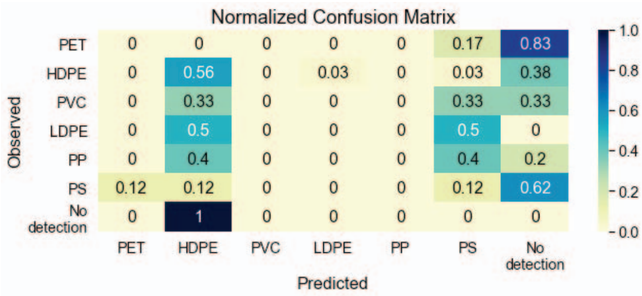

Fig. 1: Multi-class CV classification performance.

(a) PET (0%) (b) HDPE (98%) (c) PS (0%) (d) PS (60%)

Fig. 2: Examples of failed identification of plastic types. PET: (a) algae on the object, (b) object covered by deep sand. PS: (c) object in highly turbid water, (d) object in murky background.

well optimized for resource constrained devices. We use 894 underwater images that are available in public datasets [27], and cover all 6 RIC plastic types. In each image, the plastic objects have been manually annotated with a bounding box using their RIC codes. The model for object detection was trained on a GPU using 50 000 epochs and a batch size of 12.

The results are shown in Figure 1. The average accuracy for identifying the exact plastic type is around 33% with only HDPE achieving a performance higher than 50%. The higher performance is mostly due to HDPE objects having the most consistent shape and structure. Indeed, object detection can only determine materials based on the type of object and fails when the shape has changed or when the object is partially occluded. This makes object detection best suited for plastics that float and that have not been heavily degraded [28].

Some of the main challenges in detection are highlighted in Figure 2. Objects that have been a long time in the aquatic environment are difficult to recognize as they are partially assimilated with the marine ecosystem and seafloor soil (Figure. 2a and Figure. 2b). Water conditions pose another significant challenge with turbidity (Figure. 2c) and luminosity (Figure. 2d) being examples of conditions that either prevent or at least significantly decrease confidence in detection.

While there are techniques that can improve the performance of computer vision, they only partially address problem. For example, data augmentation, the use of computational transformations on training images to increase the size and quality of training data, is a common technique for improving the performance of deep learning models and can help also in underwater plastic monitoring. As the examples above highlight, plastics can undergo significant transformations in aquatic environments and covering all possible transformations in advance is next to impossible. Indeed, besides requiring heavy computational resources (unavailable underwater), a robust object detection model for characterizing materials would require a very large database that contains objects in differing angles, light and weather conditions, states of degradation as well as a thorough understanding of how to emulate these states computationally.

The key takeaway is that computer vision is sufficient for *detecting* plastic debris, but not for analysing their composition. SEAGULL targets the characterization of plastic objects and thus seeks to complement computer vision and pave way toward an approach that can simultaneously detect and analyze plastics. SEAGULL can reduce the uncertainty of collecting plastic debris and provide actionable feedback in-situ to remote operators and divers.

IV. SEAGULL Design

SEAGULL targets the accurate and robust characterization of the plastic in underwater environments with minimal resource consumption. Achieving these goals is highly challenging due to underwater environments being averse to computing and limiting what sensor data can be collected. SEAGULL achieves its goals by building on an innovative sensing pipeline that combines optical sensing with convolutional sparse coding to analyze small changes in the reflectance spectrum of plastic objects. We next explain the theoretical background of SEAGULL and then detail our solution approach.

A. Theoretical Background

Optical Sensing: SEAGULL relies on optical sensing (laser diodes or LEDs and photoreceptor) to capture reflectance patterns from different plastic objects. The basic idea is to establish a fingerprint of the reflectance properties of the object which then can be used to determine the object characteristics (material). This is similar to spectroscopy [29] that operates by establishing a spectral trace of materials by looking at light penetration and reflectance at different wavelengths. Using a broad spectrum of wavelengths would increase the weight, complexity and cost of the solution, as well as require high energy drain. SEAGULL instead focuses on a narrow spectrum of light using wavelengths that have sufficient water penetration but that are only partially absorbed by objects to collect reflectance measurements. In our experiments, we consider predominantly the red wavelength (see Sections VI-A and VI-B), but we have also carried out experiments using green wavelength (see Section VI-C). Studies on light reflection and absorption have shown these wavelengths are effective to penetrate water while remaining stable in different conditions [29], [30]. At the same time, these wavelengths have been shown to contain differing spectral responses with common plastic types [31].

Convolutional Sparse Coding for Optical Signal: A key challenge for the design of SEAGULL is how to robustly characterize underwater plastic materials. Capturing the reflectance spectrum of the object requires collecting measurements over a sufficiently long window (i.e, few seconds), but at the same time motion (e.g., currents), changes in the environment (e.g., changes in ambient luminosity due to clouds), and other environmental factors result in noise that distorts the captured light spectrum [32], [33]. To mitigate the effect of noise, SEAGULL identifies a sparse representation of the captured spectrum that characterizes the plastic, allowing the comparison of smaller parts of the overall spectrum instead of comparing the entire reflectance spectrum, while being robust to changes in the sensing conditions and environment [34]. SEAGULL achieves this by learning a sparse set of coefficients that best reconstructs the reflectance signal using the principles of sparse coding and convolutional neural networks (CNN), a.k.a. convolutional sparse coding (CSC) [35], [36]. Convolutional sparse coding is based on the idea that local patterns of input data can be encoded as convolutional dictionary filter bank under sparsity constraints (i.e., only keep the most significant representation of the data) [34]–[36]. Convolutional sparse coding is widely used to extract features and reduce dimensionality in image analysis or feature maps [36].

B. Plastic Characterization

Figure 3 shows an overview of our approach for plastic characterization. In the data pre-processing step, SEAGULL first construct a data frame of approximately 50 samples as this was found sufficient for robust identification during empirical evaluation (see Section VI-A). We preprocess the data using a FIR filter and normalize the values using standard deviation. These steps reduce noise from small movements and make the results comparable across different environments.

After pre-processing, we use convolutional sparse coding (CSC) to transform the measurements into an overcomplete and non-orthogonal space where the frame is represented as a convolution of *basis vectors* [34]. The basis vectors represent smaller constituents within the overall light spectrum and they are learned from unlabeled data which can even be collected in laboratory environments. The learned vectors are tested for best characterizing the plastic type by comparing the reconstructed light signal with the original signal. The overall set of basis vectors is known as the *codebook* and each data frame can then be represented as a weighted combination of the basis vectors in the codebook. We use the weights of the data frame as features for classifying the material of different debris. The exact size of the codebook does not matter, provided that it is set to be higher than the data dimensionality (i.e., the number of samples in a time window) to ensure it can generate an efficient and sparse representation. Besides allowing to prioritize different constituents of the overall spectrum, sparse coding can also be used to optimize resource drain. Indeed, the complexity of the model can be controlled by only considering the weights of the top-k basis vectors and setting every other activation to zero.

C. Overall Design and Implementation

SEAGULL builds on the vision of low-cost environmental sensing which has been shown to facilitate data collection and serve as catalyst for scientific studies and innovation. For example, in air quality monitoring low-cost sensors are nowadays widely adopted to increase the resolution of information that is available [37], [38]. For underwater plastics, such as technique has not existed prior to our work and SEAGULL seeks to serve as catalyst to enable low-cost underwater plastics monitoring.

SEAGULL been designed to be inexpensive and easy to implement using off-the-shelf components. Implementing SEAGULL only requires placing a light source, a control unit, and photoreceptor in a watertight container. These components can be obtained for around 10 USD and even off-the-shelf consumer devices such as smartwatches or wearables that integrate heart rate sensing could be re-purposed for plastic sensing (see Section VI-C). In our experiments, we consider a custom device that integrates red laser diodes and photoreceptors with a microcontroller (see Section V). SEAGULL has two modes of operation depending on whether a scuba diver or a drone are taking the measurements. In the former case, SEAGULL uses optical sensing integrated onto a dive computer or another wearable, asking the user to place the debris on the sensor. In the latter case, the drone uses image-based object recognition to detect debris and then navigates to the debris object before collecting measurements. These modes are illustrated in Figure 4.

V. Testbed Experiments

SEAGULL was tested in controlled benchmark evaluations, varying sensor proximity, turbulence, and turbidity conditions.

Plastic Objects: We consider all six primary RICs which are used to produce everyday plastic objects (see Section II). The performance of the optical sensing was evaluated using plastic samples that were produced using the same mould cavity and identical manufacturing process [39]. The thickness of each sample is $2\,\mathrm{mm}$, which is similar to plastics used in consumer products (e.g., plastic water bottles are $1-2\mathrm{mm}$ thick). The density of the samples varies between 0.39 and $1.5\,\mathrm{g\,cm^{-3}}$ and the weight is between 18 and $30\,\mathrm{g}$. We measure the polished area of the plastic, which is similar to those used in consumer products. Thus, differences in samples are directly proportional to their inherent material properties (material shrinkage and stiffness), and not on the shape of the objects.

Apparatus: We use a $650\,\mathrm{nm}$ red laser diode ($5\,\mathrm{mV}$, $3-5\,\mathrm{V}$) as the light source and a photo resistor to receive the reflected light. The photo resistor is connected to a Wi-Fi integrated microcontroller (M5Stack). The light intensity reflected from shining the red laser diode (see Figure 5a) on a plastic sample is measured by the photo resistor, stored locally and opportunistically uploaded to a Web server for analysis.

Experiment Setup: Measurements were taken in a controlled testbed built using a glass container ($40\,\mathrm{cm}$ x $20\,\mathrm{cm}$ x $25\,\mathrm{cm}$) covered with a non-reflective (black) lid; see Figure 5b. The container is filled with water and emulates underwater environments whereas the non-reflective lid acts as a background for the light measurements. The light sensor is taped outside the container, directly below the measured object. We use these measurements simply to control the effect of environmental variations. In Section VII we demonstrate that SEAGULL also generalizes to real-world in-the-wild deployments.

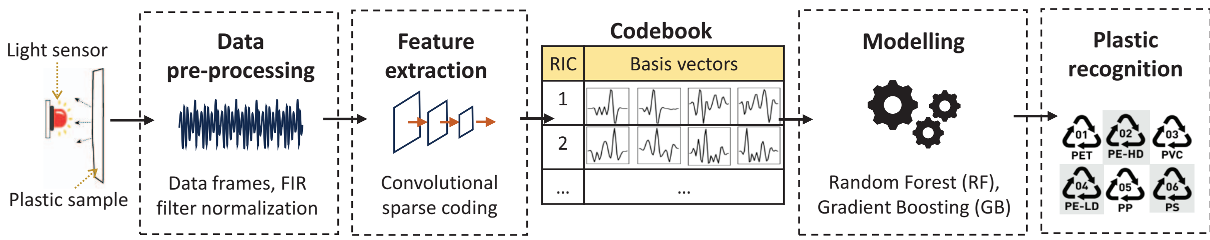

Fig. 3: Sensing pipeline for plastic characterization.

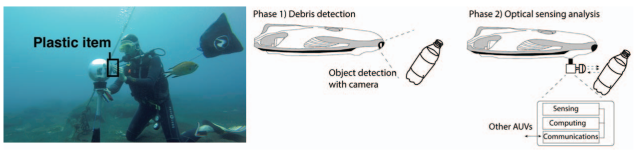

Fig. 4: SEAGULL's operation modes: (i) a SCUBA diver manually placing debris onto the sensor unit or (ii) an AUV navigating to a debris and collecting samples. Computer vision or underwater LIDAR can facilitate AUV navigation.

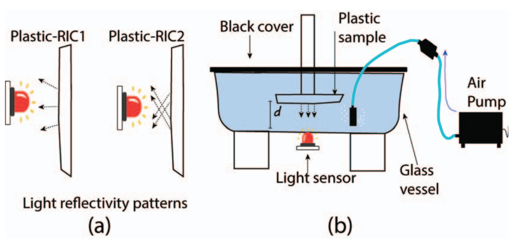

Fig. 5: Optical sensing: (a) Difference in light reflectivity patterns, (b) Testbed for underwater reflectivity sampling.

Experiment Procedures: To assess robustness of the optical sensing, we implement a testbed that allows emulating different water conditions: *turbulence*, *turbidity*, *luminosity*. High levels of water turbulence were continuously generate using two different sources: a pond aeration pump (Ubbink Air 100, $100\,\mathrm{L\,h^{-1}}$, $3\,\mathrm{W}$) and a hand mixer (House HB 1935, $200\,\mathrm{W}$). Turbidity was emulated by adding ink into the water and measured in nephelometric turbidity units (NTU) using HydroColor app [40]. We considered two turbidity conditions: drinking water ($8\,\mathrm{NTU}$) and obscure water ($80\,\mathrm{NTU}$). We tested two levels of luminosity, emulating different depths, times of day, and water visibility patterns, by switching off and blocking all sources of ambient light (dark ambient, $\approx 0\,\mathrm{lx}$), and by exposing the testbed to ambient light (ambient light, $15.5\,\mathrm{lx}$). We placed each plastic sample in turn inside the glass container and collected 12 sets of light reflectance measurements at $100\,\mathrm{Hz}$ frequency over a 90 second period. In total, we collected $648,000$ samples for six plastic types.

VI. Results

A. Optical Sensing performance

Optical Sensing Baseline: We first establish baseline values for the different plastics in a laboratory setting (on-the-ground). We then later compare these against those obtained underwater. We also compare how distance between the light receptor and plastic object affects recognition accuracy as this is essential for ensuring robust performance in different underwater conditions. The results in Figure 6a demonstrate that SEAGULL can tolerate loose contact between the plastic debris and the sensor, with the precise condition that can be tolerated depending on the environment. As the gap between the object the sensor grows, light values start to approach ambient illumination and thus, as expected, the object needs to be placed in close proximity of the sensor. In parallel, we analyze the number of samples that the sensor needs to collect from the plastics materials to identify them with high accuracy. Figure 6b shows the results obtained from sampling a plastic sample (PVC) for one minute. We find that about 50 samples are necessary to characterize a plastic type with 97.5% confidence. Measurements can be taken in less than 1 second using a sampling frequency of $100\,\mathrm{Hz}$. This is also applicable to other types of plastics. Sampling time can be further reduced by using multiple sensors simultaneously.

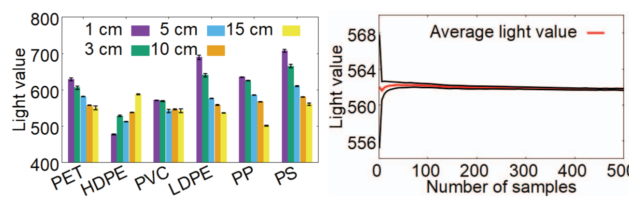

(a) (b)

Fig. 6: (a) Light characterization at different distances; (b) Amount of samples for characterization of a PVC sample.

Light Performance Underwater: We next demonstrate that the results from the on-the-ground test translate to underwater environments. Figures 7a and 7c show the difference in the plastic fingerprints under bright ambient light and dark ambient light respectively. Friedman test using different plastic types indicated statistically significant differences between the fingerprints both in the bright ($\chi^2(2) = 2500$, $p < .05$, $W = 1.0$) and dark conditions ($\chi^2(2) = 2500$, $p < .05$, $W = 1.0$). This indicates that optical sensing is effective in surface and underwater settings. As part of the experiment, we also measured the variation in light intensity as the contact between the plastic and sensor is loosened (contact, proximity-1 and proximity-2; referring to a gap of $1\,\mathrm{cm}$ and $2\,\mathrm{cm}$ between the sensor and plastic). Figures 7b and 7d show the mean absolute deviation for bright and dark ambient light conditions. In line with the surface results, we observe that the variation in measurements increases as contact is loosened.

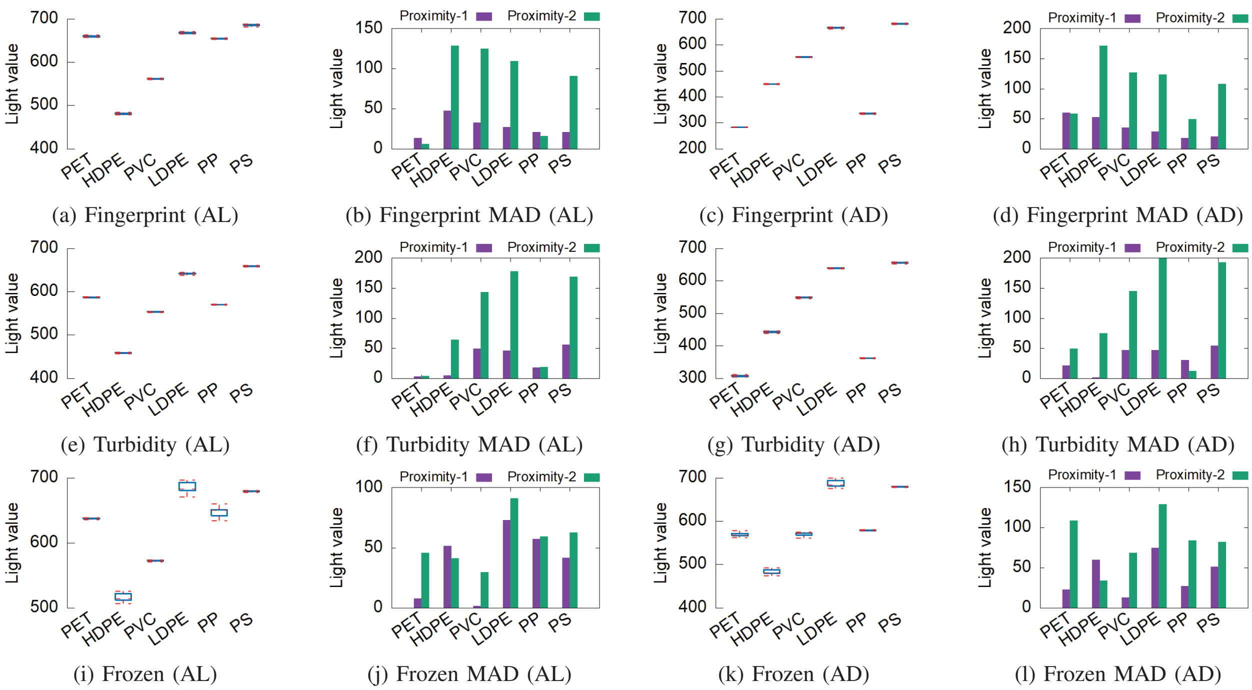

(a) Fingerprint (AL) (b) Fingerprint MAD (AL) (c) Fingerprint (AD) (d) Fingerprint MAD (AD)

(e) Turbidity (AL) (f) Turbidity MAD (AL) (g) Turbidity (AD) (h) Turbidity MAD (AD)

(i) Frozen (AL) (j) Frozen MAD (AL) (k) Frozen (AD) (l) Frozen MAD (AD)

Fig. 7: Underwater light characterization: a-d) Plastic fingerprints (Fingerprint), e-h) Influence of water turbidity (Turbidity), i-l) Influence of frozen water (Frozen). Ambient Light (AL), Ambient Dark (AD), Mean Absolute Deviation (MAD).

Classification Underwater: As light measurements can fingerprint plastics objects underwater, we next demonstrate that coarse-grained classification of plastics is possible with light samples taken underwater. We test using two simple machine learning classifiers, a Random Forest (RF) model and a Gradient Boosting (GB) model under different experimental conditions. The use of simple classifiers ensures having energy-efficient models that can be executed underwater (e.g., by a smartphone-based power unit) with minimal energy overhead. The results are shown in Table II. We separately evaluated different sensing conditions (direct, water, ice, turbulence, turbidity) and features (light reflected, luminosity, distance, water colour). As a baseline we consider an approach that considers the entire light spectrum (non-CSC) which we compare against our convolutional sparse coding (CSC). When only reflected light is used, CSC achieves around 10% higher accuracy than the use of the entire spectrum. When further information, such as distance between the sensor and the object or the ambient luminosity of the environment are included as part of the model, the performance of the full spectrum reaches similar level as the CSC. In all cases, the variance in performance for the CSC approach is small, whereas the performance of the full spectrum varies considerably across all experiments. These results demonstrate that the use of CSC significantly improves the accuracy and robustness of the plastic detection, and is a significant contributor to SEAGULL's accuracy.

B. Factors Influencing Light Performance

We next demonstrate that SEAGULL can operate in a variety of underwater environments by systematically assessing the effects of different environmental and other factors. We focus on the relative differences in fingerprints (see Figure 7) and the impact on classification performance (see Table II).

TABLE II: Classification accuracy (%) using CSC vs. full spectrum. Random Forest (RF), Gradient Boosting (GB), light reflected (r), ambient light (l), distance (d), water colour (t).

		CSC		**Full spectrum (non-CSC)**	
Test conditions		**RF**	**GB**	**RF**	**GB**
Direct	(r)	84.6	**87.0**	81.5	81.5
	(r,l)	85.2	**86.8**	83.3	83.3
Water	(r)	82.8	83.3	84.6	**85.1**
	(r,d)	83.0	83.1	**90.8**	90.4
Ice	(r)	**87.9**	87.5	74.2	76.3
	(r,l)	87.6	**87.8**	85.9	85.4
Turbulence	(r)	84.8	**86.2**	63.5	63.5
	(r,d)	85.3	**85.5**	71.9	71.4
Turbidity	(r)	**82.3**	81.7	76.7	80.7
	(r,l)	82.0	82.0	**87.0**	86.1
	(r,d)	82.4	81.9	**87.8**	86.7
	(r,t)	82.3	82.5	**85.1**	85.0
Average	(r)	84.5±2.2	**85.1±2.5**	76.1±8.1	77.4±8.4
	(r,l)	84.9±2.8	**85.5±3.1**	85.4±1.9	84.9±1.5
	(r,d)	**83.6±1.5**	83.5±1.8	83.5±10.2	82.8±10.2
	Overall	84.2±2.1	**84.6±2.4**	81.0±7.9	81.3±7.5

Water Turbidity: We analyze how water turbidity (i.e., clarity) influences sensing of plastics underwater. Relative differences in light values are preserved even in high turbidity conditions (80 NTU) and holds under both bright (Figure 7e) and dark (Figure 7g) ambient light. Friedman test verified that the differences in fingerprints were significant (with a large effect) both for bright ($\chi^2(2) = 2500$, p $<$ .05, $W = 1.0$) and dark ($\chi^2(2) = 2500$, p $<$ .05, $W = 1.0$) environments. The analysis of the interaction between turbidity and distance (see

Figures 7f and 7h) indicates that high turbidity (80 NTU) does not introduce significant variations for recognizing plastics compared to a clear water baseline (8 NTU).

Water State: Since water can change to a different state based on environmental conditions, we also evaluate our approach in conditions where water freezes (i.e., changes to a solid state). We placed the testbed in a freezer (temperature $-20\,°C$) until the water was frozen and we then proceeded to identify plastics trapped in the frozen water. As before, we carried out the experiments using the two distances between the plastic object and the photoreceptor (1 cm and 2 cm). Figures 7i and 7k show the results for ambient and dark light conditions, respectively. We observe that light is able to penetrate ice and can be used to identify the plastics. The relative fingerprint values are preserved, as also confirmed by Friedman test (bright: $\chi^2(2) = 2500$, $p < .05$, $W = 1.0$, dark: $\chi^2(2) = 2500$, $p < .05$, $W = 1.0$). Figures 7j and 7l show the variations in light measurements for different distances, demonstrating that the results are comparable to non-frozen settings and that plastics can be recognized even when trapped in ice.

Water Turbulence: In many underwater environments water is undergoing constant motion due to wind, currents, and other factors. We next analyze the influence of water motion in the sensing process. We use a water pump to generate turbulence, and evaluate the effect of the distance between the object and the photoreceptor as before. Figure 8 shows the results. Water motion generally increases variation in the measurements, with the distance being larger as the distance between the photoreceptor and the plastic object increases. However, the relative differences in fingerprints are preserved, suggesting that the motion has negligible effect on recognition performance. Friedman test shown that differences in fingerprints remained significant for all distances (1 cm: $\chi^2(2) = 2307$, $p < .05$, $W = 0.92$; 2 cm: $\chi^2(2) = 2355$, $p < .05$, $W = 0.94$). Looking back at the classification results in Table II, this result best demonstrates the power of convolutional sparse coding. Indeed, the performance of the baseline suffers most in turbulent conditions whereas the CSC achieves similar performance as in calm conditions. This highlights how the use of sparse representations is necessary for mitigating motion artifacts and other sources of noise in the light signals.

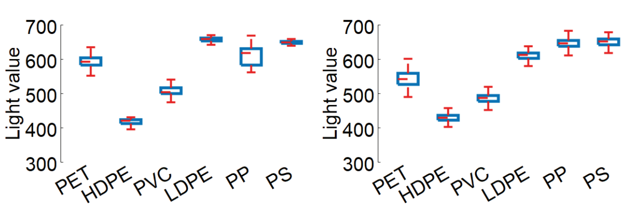

(a) Proximity: 1 cm (b) Proximity: 2 cm

Fig. 8: Water turbulence affecting characterization.

Other Plastics: Thus far our experiments have focused on a fixed set of plastics. We next demonstrate that the results generalize also to other plastics. Table III describes a list of additional plastics samples that are considered in our experiments and Figure 9 shows the results. Friedman test shows significant differences with a large effect for bright ($\chi^2(2) = 2500$, $p < .05$, $W = 1.0$) and dark ($\chi^2(2) = 2500$, $p < .05$, $W = 1.0$) conditions. Posthoc comparisons (Dunn-Bonferroni) verify that these hold for all plastics. This suggests that other plastic types can be characterized and different variations of plastics from the same family can be distinguished.

TABLE III: Additional plastic types in experiments.

Id	Acron.	Plastic name	Color
1	POM	Polyoxymethylene	black
2	PMMA	Polymethyl methacrylate	transparent
3	PSU	Polysulfone	transparent
4	PP+GF	Polypropylene	black
5	PBT+GF	Glass-reinforced polybutylene terephthalate	black
6	PPA+GF	Polyamides	black
7	TPE-S	Thermoplastic elastomer	pink
8	PBT	Polybutylene terephthalate	white
9	PA6	polyamide	green
10	PA66+GF	Glass-reinforced polyamide	black
11	PC	Polycarbonate	transparent
12	PC/ABS	Blend polycarbonate	white
13	PPS+GF	Glass-reinforced polyphenylene sulfide	black
14	ABS	Acrylonitrile butadiene styrene	white
15	EVA	Ethylene vinyl acetate	white

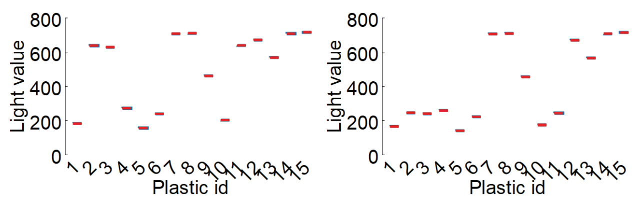

(a) Ambient light (b) Ambient dark

Fig. 9: Light characterization of a larger variety of plastics with different properties and colors.

Plastic color: Finally, we analyze how color influences the characterization of plastics. To accomplish this, we divide the plastics by color and analyze the differences in fingerprint within and between the groups. The largest groups comprise of black and transparent samples. For black plastic samples, the differences in fingerprints are preserved and remain significant (Friedman test: $\chi^2(2) = 2462$, $p < .05$, $W = 0.98$). Posthoc comparisons (Dunn-Bonferroni) confirm that the individual plastics can equally be separated within this category. In turn, transparent plastics show more variations in the fingerprints, and luminosity affect the extent of these variations. Thus optimally the measurements should be collected against a sufficiently dark and consistent background.

C. Repurposing Off-the-Shelf Sensors

We next use the PPG (photoplethysmogram) sensor of a Samsung Gear S3 Frontier smartwatch to assess whether off-the-shelf consumer hardware can be repurposed for detection. The smartwatch integrates two green LED lights and a photoreceptor. Figure 10 shows the results of the underwater experiments. We observe that different materials have different reflectance, and that the relative differences are preserved for both ambient light and darkness conditions. Kruskal-Wallis

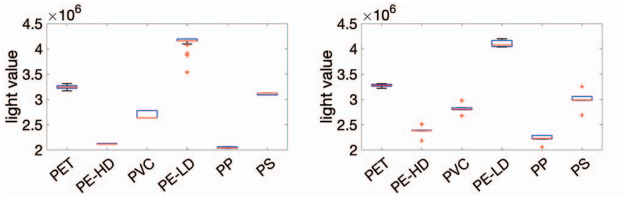

(a) Ambient light (b) Ambient dark

Fig. 10: Underwater plastics green light sensing.

test using luminosity and plastic type as experimental conditions showed significant differences for ambient ($\chi^2 = 9176$, $\eta^2 = 0.89$, p$<$ .001) and darkness ($\chi^2 = 16562$, $\eta^2 = 0.946$, p$<$ .001). Posthoc comparisons (Dunn-Bonferroni) verified that the differences were statistically significant. This suggests that light sensors can be used for plastic identification.

D. Water Stability Detection

The results thus far have demonstrated that water motion increases variance in the light reflectance measurements, even when convolutional sparse coding is robust against such motion. However, our experiments focused on constant motion and in practice there can be variations in the water motion that also affect quality. In these cases, a potential way to further enhance performance is to detect periods that are sufficiently stable and only use measurements from these periods to form the fingerprint. We next analyze how accelerometers can be used to characterize water motion levels and potentially enhance the performance of SEAGULL.

We place an accelerometer on the water surface and consider measurements in three conditions: i) calm water (no water motion is induced), ii) pump water and iii) mixed water. We then estimate the overall motion by calculating the variance of the three axes over a period of time. Figure 11 shows the overall motion captured in each condition. As expected, we observe that calm water does not affect accelerometer measurements, whereas water motion induced by the pump is moderate compared to that induced by the mixer. The results also support the use of accelerometer to characterize water motion. For example, an accelerometer can be used to assign a *quality score* on the light measurements based on the water motion, and only including measurements that have sufficiently high quality score. Naturally, this means that forming the data frame can take longer and hence the sensing time would depend on the environment where the measurements are taken. The quality score can be simply calculated by examining the variation of accelerometer measurements as this provides an indication of the impact of turbulence during sampling. A greater variation in the intensity of the accelerometer increases the likelihood of optical measurements distortion and reduces the quality of the measurements. Note that we do not expect water to be still, rather that water motion is consistent. Most water motion is periodic in nature which means that even during heavy waves or currents there are regular periods where the motion is consistent and that samples can be taken reliably.

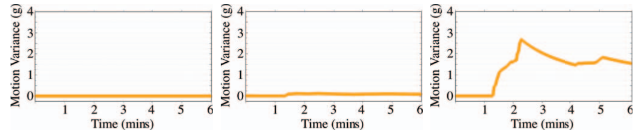

(a) Calm water (b) Pump water (c) Mixer water

Fig. 11: Water stability characterization.

Method	Cost	Effort	Analysis Type	Analysis
Infrared Spectroscopy	High	High	Composition	Lab-based
Computer Vision	Low	Low	Detection	In-situ or on surface
Visual Surveys	Medium	Medium	Detection, coarse composition	On surface, after data collection
SEAGULL	**Low**	**Low**	**Composition**	**In-Situ**

Fig. 12: Comparing approaches for underwater plastic analysis

E. Comparison to Other Techniques

SEAGULL has been designed as a low-cost solution for analysing the composition of underwater plastics. It overcomes the limitations of current techniques while enabling in-situ analysis of debris, eliminating the need to transport objects to a laboratory for analysis. Figure 12 demonstrates these points by summarizing different techniques utilised for plastic analysis. Infrared spectroscopy has the best overall accuracy, but suffers from a high price point and significant delay between the analysis and collection of measurements. Computer vision, in contrast, is limited to analysing the objects based on their visual appearance and only work on objects that are intact. Finally, visual surveys basically fall in between these approaches, requiring laboratory analysis for detailed analysis or only providing coarse information based on the visual appearance of the materials. These methods also suffer from severe biases, e.g., aerial surveys only capture plastics that float. SEAGULL offers a low-cost alternative to obtain information directly in the underwater environment. Samples that are complex to analyze, e.g., due to accumulation of silt or marine growth, can still be taken back to laboratory for further analysis, allowing SEAGULL to be used as a way to perform early analysis and scale-up data collection.

VII. Field Validation

Thus far we have shown that SEAGULL provides a promising solution for detecting plastic debris and identifying the composition of detected plastics. Next, we demonstrate that the results translate to real-world underwater environments that contain a combination of different turbidity, turbulence, water density, and other factors. We provide benchmark results for both sweet and salt water environments demonstrating that the lab results generalize to the field. This section also serves as an example of the two modes of operation of SEAGULL, as explained in Section IV-C.

A. Scuba Diving Experiment - Ocean

We assess the performance of SEAGULL by using it as part of a recreational scuba diving activity. We design a pressure-resistant prototype station, which is deployed underwater at

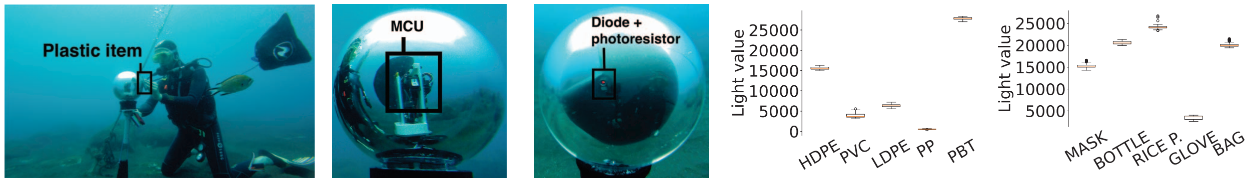

(a) (b) (c) (d) (e)

Fig. 13: SEAGULL in sea: (a) Scuba diver passing the collected plastic marine pollutant for characterization in front of the station; (b) Rear view; (c) Frontal view; (d) RIC characterization; and (e) Litter characterization.

greater depths. Divers can then rely on it to confirm collected debris properties before taking it back to the surface.

Plastics Monitoring Station: We design the station using a waterproof dome made from acrylic, mounted on the PVC pipe stand as well as lead diving belt weights (see Figure 13). Such approach allowed the device to stay in fixed place while swinging during the strong swells [15]. Dome encompassed custom-designed and 3D-printed mounting for Raspberry Pi Zero W, $1750\,\mathrm{mAh}$ Li-Po rechargeable battery (see Figure 13b), as well as the laser diode and photoresistor used in previous experiments (see Figure 13c). Additional black background was placed around the laser module to reduce the light scattering. We used the same plastic samples described in our controlled experiments and the same products used in our river deployment (see Section VII-B). RIC item 5 (PP) was used in black color as the complementary litter material (face mask, PP) was in color. Five from six items from each kind were used due to the amount of air left in the scuba tank, as the experiment was conducted at the end of the dive, respecting the $50\,\mathrm{bars}$ of air margin for returning to the dive center. At the depth of $10\,\mathrm{m}$, each plastic item was placed in front of the sensing station for $30\,\mathrm{s}$. As previously, $1\,\mathrm{cm}$ distance between the laser/photo receptor inside the dome and the outside plastic items was used. All items were safely collected after the underwater deployment using the SCUBA diving bag (see Figure 13a).

Results: Figures 13d and 13e show the results. Light values on y axis are with different scale compared to laboratory and river experiments (Figures 10b and 14b) due to usage of analogue to digital conversion and different MCU (Raspberry Pi W Zero). Thus, prior normalization was required. When comparing RIC (Figure 13d) to litter samples (Figure 13e), the laboratory samples are comparable to the litter samples, e.g. readings of PVC sample and the glove, or HDPE laboratory sample and grocery bag. However, the water environment and color affects the readings, providing discrepancies. When comparing litter items sampled in salt waters (see Figure 13e) against same items in sweet waters (see Figure 15a), mostly transparent litter samples (e.g., Plastic Bottle, Rice package and Grocery bag), fall within similar trend. Kolmogorov-Smirnov test for plastic litter items between all pairs (river-sea, river-controlled, sea-controlled) indicates no statistical significance ($p > .05$). Similarly, all RIC pairs (sea-$1\mathrm{cm}$ controlled, sea-$3\mathrm{cm}$ controlled) provide no statistical significance ($p > .05$), demonstrating the shared data similarities. Results indicate plausible characterization of plastics in sea, suggesting SEAGULL as being robust to operate at greater depths.

B. ROV Experiment - River

SEAGULL was integrated with a remotely-operated underwater vehicle and performing a small-scale field evaluation in a river that is mildly polluted and has low visibility. The measurements were taken near the shore. The water was mostly calm during the experiments, but occasionally water jets caused turbulence. Thus, the conditions in the river covered most of the controlled factors analyze previously.

Underwater Vehicle Integration: We have implemented a proof-of-concept prototype that integrates the optical sensing of SEAGULL with a PowerVision AUV PowerRay ($3800g$) – a reasonably priced (around 2700 USD) off-the-shelf drone that offers around 4 hours of dive time. The optical sensing components are placed into a glass container together with a battery pack of $4000\,\mathrm{mAh}$ ($14.8\,\mathrm{Wh}$) capacity. The container is then attached to the AUV. Off-the-shelf AUVs have specialized locations to plug components and we used the frontal location below the AUV, as shown in Figure 14a. In total, the sensing components weigh $970\,\mathrm{g}$, which is light enough for the drone to carry. The battery pack allows the components to operate continuously for about 27 hours, well beyond the dive time of the drone itself. We note that it is possible to make the components much lighter, e.g., using a smartwatch would reduce the weight by a factor of about 5 and increase the operational time to over 100 hours. Our focus was not on optimizing the system design, but on designing a rapid prototype that could be used to test the performance of the optical sensing in the real-world.

Field Experiments: We conduct a small-scale field test using the drone in a river and common plastic products that have been discarded and that are representative of most common (RIC) plastic types. The objects are shown in Figure 14b and include A: PET plastic bottle, B: HPDE plastic bag, C: PVC plastic gloves, D: PP face mask, E: PS food packing for green beans and F: PS food packing for rice. We measured the light reflectance of the whole object by dividing the object into $1\,\mathrm{cm}^2$ areas and measured the light reflectance from each of these squared areas for $10\,\mathrm{s}$. The plastic products were then tied to weights and submerged in the river. This was done to keep the products floating without being dragged away by the water current, and to facilitate their extraction at the end of the experiment. Measurements were taken from about a few meters depth with environment luminosity of average $11\,000\,\mathrm{lx}$. In the experiment, we manually navigate the drone to the products and use optical sensing to classify the samples in a sequential manner. We verified that differences in light intensity were statistically significant (Kruskal-Wallis test: $\chi^2 = 2917$, $\eta^2 = 0.97$, p< 0.05) across all plastics.

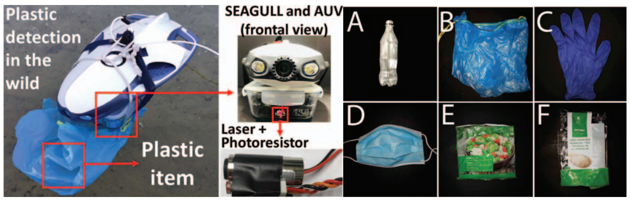

(a) (b)

Fig. 14: (a) Prototype of AUV integrated with SEAGULL, (b) Plastic products used in the underwater tests.

Optical Sensing Performance: We measure the stability of the light intensity measurements taken underwater to analyze their variability and compare them against those taken in the controlled experiments. Figure 15a shows the results. The relative characterization of objects is preserved and thus robust classification remains possible. This can change however based on the variability of the light measurements, caused due to higher distance to the target, water motion and surface characteristics of the plastic objects. Indeed, solid plastic objects, such as bottle, have lower variance than objects with malleable surfaces, such as plastic bags, whose shape is affected by water motion. We also repeated the experiment on the ground at $1\,\mathrm{cm}$ distance from the objects to verify that the differences remained consistent with the underwater tests. The Figure 15b results align with previous results with the lack of motion resulting in lower variance in the measurements. We note changes in reflected light values for certain materials, consistent with the findings discussed in Section VI-A. These results demonstrate the need to consider ambient light intensity when classifying these materials.

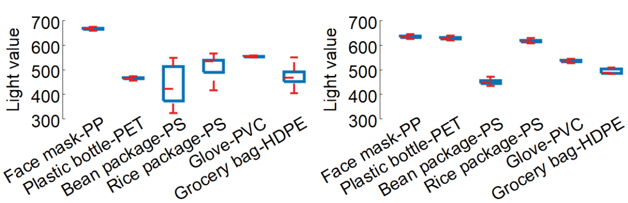

(a) Underwater (in the field) (b) Baseline

Fig. 15: SEAGULL performance in sweet water: (a) Classification in the field, (b) Baseline (proximity: $1\,\mathrm{cm}$).

VIII. Discussion

Applicability: Vision-based methods can assist divers and ROVs to detect underwater plastic debris, but fail to provide information on the plastic type. Prior to our work, determining the material requires retrieving the debris, taking them to a lab, and analyzing them using dedicated measurement tools. SEAGULL is the first solution to enable in-situ analysis of the plastic composition. We have demonstrated how it can be integrated both to underwater drones and equipment carried by scuba divers. Our long-term vision sees our work as a key component for enabling large-scale mapping of underwater plastics. Naturally further work is needed to enable this vision, e.g., to improve the overall system design (e.g., in terms of form factor and underwater casing). We could also envision SEAGULL to be embedded into moving buoys and other aquatic infrastructure to monitor the distribution and characteristics of plastics, but this also requires to investigate in parallel, new mechanisms that automatically probe samples from the surroundings. For instance, buoys with robotic arms or retractable sensors.

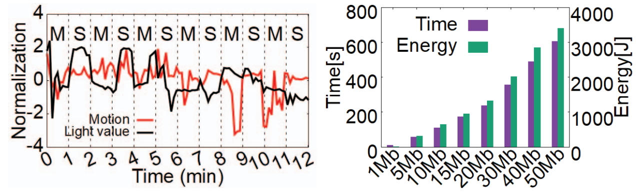

(a) (b)

Fig. 16: (a) Effect of motion on reflected light (y axis only), M: Moving, S: Still; (b) Video processing time and energy on the Raspberry PI Zero.

Room for improvement: SEAGULL identifies characteristics of plastic debris as samples are probed. Scuba divers can place objects directly on the optical sensor which offers an easy way to analyze debris found in underwater environments, whereas in the future we could expect ROVs or even AUVs to integrate actuators that allow grabbing the debris, placing it on a sensor, and placing it in a removal container that allows removing the debris. Note that this is only needed for analysing the *composition* of the plastic, and the presence of plastics can be detected from a longer distance, e.g., using computer vision, naked eye, or even acoustic sensing. The next challenge relates to underwater optical measurements being contaminated by noise. We demonstrated that the use of convolutional sparse coding allows obtaining a representation that is more robust to noise, significantly improving the performance of our system. Loose contact between the debris and sensor is one of the main sources of noise, and the integration of sparse coding thus also helps performing the analysis in underwater environments. Overall, SEAGULL significantly reduces the complexity of mapping plastic pollutants as it enables analysing the composition of plastic debris in-situ. Another key challenge is to design suitable prototypes to further increase the sensors' operational range. For example, currently we can operate at recreational scuba diving depths (up to 30 meters). At greater depths, better designs that account for the increase in pressure are needed.

IX. Related work

Marine litter can be detected by observers on-board vessels, using diving or towing surveys where a diver is taken over a target area in a predetermined pattern and speed. Bottom trawls also have been used for investigating seafloor litter but these can be destructive to aquatic ecosystems. Existing works to automatize the process have largely relied on image recognition approaches to identify different material properties, including plastic [41]. Some alternatives have also been proposed, such as the use of Near-infrared (NIR) sensors [42], [43] but these are ill-suited for aquatic environments due to the signals being poor at penetrating water and typically are used in a lab on aquatic collected samples. Other ground-based techniques include laser and multi-directional, multi-spectral LED illumination of materials [44], the use of side-scan sonar for detecting macro-litter and other objects [45]. These approaches are difficult to adopt in underwater field-use, and they are mostly geared toward detecting items rather than identifying their composition. Our work offers an innovative solution that performs robustly in underwater environments and can be adopted by scuba divers and off-the-shelf AUVs.

Non-contact-based sampling relies on external sensors, e.g., hyperspectral cameras and sensorless Wi-Fi, to identify objects [46]. Non-contact based solutions have been extensively studied but are highly vulnerable to the operating environment [47] and require sufficient computational resources to be available [48], making them impractical for underwater settings. Wireless sensing also can be used to recognize object materials, e.g., liquids [49]. Non-contact techniques along with aerial drones have been studied to detect floating debris [50]. In parallel to this, contact-based sensors have been studied to characterize object materials. Common material sensing relies on different light spectrum and measures reflection or absorption at different frequencies. Examples range from the use of green light for inorganic material detection [51] and red light for drink spiking detection [52] to the use of near-infrared to facilitate medicine adherence [53]. Other contact techniques that use RFID tags have also been explored [54]. Unlike others, we offer a low-cost solution that can operate robustly across different underwater environments.

X. Summary

We contributed SEAGULL, a novel pervasive sensing approach for monitoring underwater plastics using a light (LED) sensing solution that simultaneously detects and classifies plastic debris according to their material (resin identification code - RIC). We demonstrated that SEAGULL correctly distinguishes between the main plastic categories (over 85% accuracy), is able to operate robustly against diverse water conditions (turbulence, turbidity, luminosity), works with different sensing resolutions, and can operate even in frozen water. We also demonstrated the practicality of SEAGULL by integrating it with a ROV and recreational SCUBA diving activity, conducting field tests in both the river and sea-based deployments, showcasing the performance of SEAGULL and how it translates to real in-the-wild environments. Our work takes an important first step in providing a low-cost solution that can produce actionable, detailed, and timely information about the extent and nature of plastic pollutants.

Acknowledgements

This research was financed by European Social Fund via "ICT programme" measure, the Academy of Finland (grant: 339614), and the Nokia Foundation (grant: 20220138). Additional funding provided by FCT project INTERWHALE - Advancing Interactive Technology for Responsible Whale-Watching (grant: PTDC/CCI-COM/0450/2020). Study had the support of FCT through the strategic project UIDB/04292/2020 awarded to MARE, through project LA/P/0069/2020 granted to the Associate Laboratory ARNET.

References

[1] F. Thevenon, C. Carroll, and J. Sousa (Eds.), "Plastic debris in the ocean: the characterization of marine plastics and their environmental impacts," International Union for Conservation of Nature, Situation Analysis Report, 2015.

[2] R. E. Schnurr, V. Alboiu, M. Chaudhary, R. A. Corbett, M. E. Quanz, K. Sankar, H. S. Srain, V. Thavarajah, D. Xanthos, and T. R. Walker, "Reducing marine pollution from single-use plastics (SUPs): A review," *Marine Pollution Bulletin*, vol. 137, pp. 157 – 171, 2018.

[3] J. C. Prata, A. L. Silva, T. R. Walker, A. C. Duarte, and T. Rocha-Santos, "COVID-19 pandemic repercussions on the use and management of plastics," *Environmental Science & Technology*, vol. 54, no. 13, pp. 7760–7765, 2020.

[4] M. Rodrigues, N. Abrantes, F. Gonçalves, H. Nogueira, J. Marques, and A. Gonçalves, "Impacts of plastic products used in daily life on the environment and human health: What is known?" *Environmental Toxicology and Pharmacology*, vol. 72, p. 103239, 2019.

[5] A. L. Andrady, "The plastic in microplastics: A review," *Marine Pollution Bulletin*, vol. 119, no. 1, pp. 12–22, 2017.

[6] C. Schönlau, T. M. Karlsson, A. Rotander, H. Nilsson, M. Engwall, B. van Bavel, and A. Kärrman, "Microplastics in sea-surface waters surrounding sweden sampled by manta trawl and in-situ pump," *Marine pollution bulletin*, vol. 153, p. 111019, 2020.

[7] A. Spengler and M. F. Costa, "Methods applied in studies of benthic marine debris," *Marine Pollution Bulletin*, vol. 56, no. 2, pp. 226–230, 2008.

[8] P. G. Ryan, C. J. Moore, J. A. van Franeker, and C. L. Moloney, "Monitoring the abundance of plastic debris in the marine environment," *Philosophical Transactions of the Royal Society B: Biological Sciences*, vol. 364, no. 1526, pp. 1999–2012, 2009.

[9] T. van Emmerik and A. Schwarz, "Plastic debris in rivers," *Wiley Interdisciplinary Reviews: Water*, vol. 7, no. 1, p. e1398, 2020.

[10] J.-L. Xu, K. V. Thomas, Z. Luo, and A. A. Gowen, "FTIR and Raman imaging for microplastics analysis: State of the art, challenges and prospects," *TrAC Trends in Analytical Chemistry*, vol. 119, p. 115629, 2019.

[11] C. A. Choy, B. H. Robison, T. O. Gagne, B. Erwin, E. Firl, R. U. Halden, J. A. Hamilton, K. Katija, S. E. Lisin, C. Rolsky, and K. S. Van Houtan, "The vertical distribution and biological transport of marine microplastics across the epipelagic and mesopelagic water column," *Scientific Reports*, vol. 9, no. 1, pp. 1–9, 2019.

[12] M. Fulton, J. Hong, M. J. Islam, and J. Sattar, "Robotic detection of marine litter using deep visual detection models," in *Proceedings of the International Conference on Robotics and Automation*. IEEE, 2019, pp. 5752–5758.

[13] M. Valdenegro-Toro, "Submerged marine debris detection with autonomous underwater vehicles," in *Proceedings of the International Conference on Robotics and Automation for Humanitarian Applications*. IEEE, 2016, pp. 1–7.

[14] C. van Lieshout, K. van Oeveren, T. van Emmerik, and E. Postma, "Automated river plastic monitoring using deep learning and cameras," *Earth and Space Science*, vol. 7, no. 8, p. e2019EA000960, 2020.

[15] M. Radeta, A. Zuniga, N. H. Motlagh, M. Liyanage, R. Freitas, M. Youssef, S. Tarkoma, H. Flores, and P. Nurmi, "Deep learning and the oceans," *Computer*, vol. 55, no. 5, pp. 39–50, 2022.

[16] M. Geraeds, T. van Emmerik, R. de Vries, and M. S. bin Ab Razak, "Riverine plastic litter monitoring using unmanned aerial vehicles (uavs)," *Remote Sensing*, vol. 11, no. 17, p. 2045, 2019.

[17] G. Jakovljevic, M. Govedarica, and F. Alvarez-Taboada, "A deep learning model for automatic plastic mapping using unmanned aerial vehicle (uav) data," *Remote Sensing*, vol. 12, no. 9, p. 1515, 2020.

[18] L. D. Stone, C. M. Keller, T. M. Kratzke, and J. P. Strumpfer, "Search analysis for the underwater wreckage of Air France Flight 447," in *Proceedings of the International Conference on Information Fusion*. IEEE, 2011, pp. 1–8.

[19] R. R. Murphy, K. L. Dreger, S. Newsome, J. Rodocker, E. Steimle, T. Kimura, K. Makabe, F. Matsuno, S. Tadokoro, and K. Kon, "Use of remotely operated marine vehicles at Minamisanriku and Rikuzentakata Japan for disaster recovery," in *2011 IEEE International Symposium on Safety, Security, and Rescue Robotics*. IEEE, 2011, pp. 19–25.

[20] G. Mordecai, P. A. Tyler, D. G. Masson, and V. A. Huvenne, "Litter in submarine canyons off the west coast of portugal," *Deep Sea Research Part II: Topical Studies in Oceanography*, vol. 58, no. 23-24, pp. 2489–2496, 2011.

[21] F. Pita and A. Castilho, "Separation of plastics by froth flotation. the role of size, shape and density of the particles," *Waste Management*, vol. 60, pp. 91–99, 2017.

[22] J. N. Hahladakis, C. A. Velis, R. Weber, E. Iacovidou, and P. Purnell, "An overview of chemical additives present in plastics: Migration, release, fate and environmental impact during their use, disposal and recycling," *Journal of Hazardous Materials*, vol. 344, pp. 179–199, 2018.

[23] Medium, "Plastix creates new material from used maritime gear," 2021, [accessed: 2023-10]. [Online]. Available: https://medium.com/2030magazine/plastix-creates-new-material-from-ghost-nets-d9ce9ee4ca83

[24] K. Zhang, A. H. Hamidian, A. Tubić, Y. Zhang, J. K. Fang, C. Wu, and P. K. Lam, "Understanding plastic degradation and microplastic formation in the environment: A review," *Environmental Pollution*, vol. 274, p. 116554, 2021.

[25] T. J. Langlois, E. S. Harvey, B. Fitzpatrick, J. J. Meeuwig, G. Shedrawi, and D. L. Watson, "Cost-efficient sampling of fish assemblages: comparison of baited video stations and diver video transects," *Aquatic Biology*, vol. 9, no. 2, pp. 155–168, 2010.

[26] M. Sandler, A. Howard, M. Zhu, A. Zhmoginov, and L.-C. Chen, "Mobilenetv2: Inverted residuals and linear bottlenecks," in *Proceedings of the IEEE Conference on Computer Vision and Pattern Recognition*, 2018, pp. 4510–4520.

[27] J. Hong, M. Fulton, and J. Sattar, "Trashcan: A semantically-segmented dataset towards visual detection of marine debris," *arXiv preprint arXiv:2007.08097*, 2020.

[28] S. Almeida, M. Radeta, T. Kataoka, J. Canning-Clode, M. Pessanha Pais, R. Freitas, and J. G. Monteiro, "Designing unmanned aerial survey monitoring program to assess floating litter contamination," *Remote Sensing*, vol. 15, no. 1, 2023.

[29] D. Bhargava and D. W. Mariam, "Light penetration depth, turbidity and reflectance related relationship and models," *ISPRS Journal of Photogrammetry and Remote Sensing*, vol. 46, no. 4, pp. 217–230, 1991.

[30] P. Eloranta, "Light penetration in different types of lakes in central finland," *Ecography*, vol. 1, no. 4, pp. 362–366, 1978.

[31] M. Moshtaghi, E. Knaeps, S. Sterckx, S. Garaba, and D. Meire, "Spectral reflectance of marine macroplastics in the vnir and swir measured in a controlled environment," *Scientific Reports*, vol. 11, no. 1, p. 5436, 2021.

[32] M. Sharifzadeh and M. Ahmadirad, "Performance analysis of underwater wireless optical communication systems over a wide range of optical turbulence," *Optics Communications*, vol. 427, pp. 609–616, 2018.

[33] B. Askarian, K. Jung, and J. W. Chong, "Monitoring of heart rate from photoplethysmographic signals using a Samsung Galaxy Note8 in underwater environments," *Sensors*, vol. 19, no. 13, p. 2846, 2019.

[34] S. Bhattacharya, P. Nurmi, N. Hammerla, and T. Plötz, "Using unlabeled data in a sparse-coding framework for human activity recognition," *Pervasive and Mobile Computing*, vol. 15, pp. 242–262, 2014.

[35] H. Bristow, A. Eriksson, and S. Lucey, "Fast convolutional sparse coding," in *Proceedings of the IEEE Conference on Computer Vision and Pattern Recognition*, 2013, pp. 391–398.

[37] N. H. Motlagh, E. Lagerspetz, P. Nurmi, X. Li, S. Varjonen, J. Mineraud, M. Siekkinen, A. Rebeiro-Hargrave, T. Hussein, T. Petaja, M. Kulmala, and S. Tarkoma, "Toward massive scale air quality monitoring," *IEEE Communications Magazine*, vol. 58, no. 2, pp. 54–59, 2020.

[36] B. Wohlberg, "Efficient convolutional sparse coding," in *Proceedings of the IEEE Conference on Acoustics, Speech and Signal Processing*. IEEE, 2014, pp. 7173–7177.

[38] F. Concas, J. Mineraud, E. Lagerspetz, S. Varjonen, X. Liu, K. Puolamäki, P. Nurmi, and S. Tarkoma, "Low-cost outdoor air quality monitoring and sensor calibration: A survey and critical analysis," *ACM Transactions on Sensor Networks*, vol. 17, no. 2, pp. 1–44, 2021.

[39] M. shop, *Plastic samples*. ", 2022. [Online]. Available: https://www.materialsampleshop.com/products/plastics-sample-set

[40] T. Leeuw and E. Boss, "The hydrocolor app: Above water measurements of remote sensing reflectance and turbidity using a smartphone camera," *Sensors*, vol. 18, no. 1, p. 256, 2018.

[41] K. Tanaka, Y. Mukaigawa, T. Funatomi, H. Kubo, Y. Matsushita, and Y. Yagi, "Material classification using frequency-and depth-dependent time-of-flight distortion," in *Proceedings of the IEEE Conference on Computer Vision and Pattern Recognition*, 2017, pp. 79–88.

[42] W. Van Den Broek, D. Wienke, W. Melssen, and L. Buydens, "Plastic material identification with spectroscopic near infrared imaging and artificial neural networks," *Analytica Chimica Acta*, vol. 361, no. 1-2, pp. 161–176, 1998.

[43] H. Masoumi, S. M. Safavi, and Z. Khani, "Identification and classification of plastic resins using near infrared reflectance," *International Journal of Mechanical, Aerospace, Industrial, Mechatronic and Manufacturing Engineering*, vol. 6, no. 5, pp. 213–220, 2012.

[44] M. Sato, S. Yoshida, A. Olwal, B. Shi, A. Hiyama, T. Tanikawa, M. Hirose, and R. Raskar, "Spectrans: Versatile material classification for interaction with textureless, specular and transparent surfaces," in *Proceedings of the ACM Conference on Human Factors in Computing Systems*. ACM, 2015, pp. 2191–2200.

[45] R. W. Simm and R. B. Kidd, "Submarine debris flow deposits detected by long-range side-scan sonar 1,000-kilometers from source," *Geo-marine letters*, vol. 3, no. 1, pp. 13–16, 1983.

[46] Y. Cho, N. Bianchi-Berthouze, N. Marquardt, and S. J. Julier, "Deep thermal imaging: Proximate material type recognition in the wild through deep learning of spatial surface temperature patterns," in *Proceedings of the CHI Conference on Human Factors in Computing Systems*. ACM, 2018, p. 2.

[47] G. Schwartz and K. Nishino, "Recognizing material properties from images," *IEEE Trans. on Pattern Analysis and Machine Intelligence*, 2019.

[48] H.-S. Yeo, J. Lee, A. Bianchi, D. Harris-Birtill, and A. Quigley, "Specam: sensing surface color and material with the front-facing camera of a mobile device," in *Proceedings of the International Conference on Human-Computer Interaction with Mobile Devices and Services*. ACM, 2017, p. 25.

[49] S. Yue and D. Katabi, "Liquid testing with your smartphone," in *Proceedings of the International Conference on Mobile Systems, Applications, and Services*. ACM, 2019, pp. 275–286.

[50] K. Moy, B. Neilson, A. Chung, A. Meadows, M. Castrence, S. Ambagis, and K. Davidson, "Mapping coastal marine debris using aerial imagery and spatial analysis," *Marine Pollution Bulletin*, vol. 132, pp. 52–59, 2018.

[51] A. Zuniga, P. Nurmi, and H. Flores, "Ripe or rotten? low-cost produce quality estimation using reflective green light sensing," *IEEE Pervasive Computing*, 2021.

[52] Z. Yin, M. Liyanage, A. Zuniga, P. Nurmi, and H. Flores, "Hedgehog: Detecting drink spiking on wearables," in *Proceedings of the International Workshop on Mobile Computing Systems and Applications*, 2023, pp. 61–67.

[53] S. Klakegg, J. Goncalves, C. Luo, A. Visuri, A. Popov, N. van Berkel, Z. Sarsenbayeva, V. Kostakos, S. Hosio, S. Savage, and A. Bykov, "Assisted medication management in elderly care using miniaturised near-infrared spectroscopy," *Proceedings of the ACM Interactive, Mobile, Wearable and Ubiquitous Technologies*, vol. 2, no. 2, p. 69, 2018.

[54] U. Ha, Y. Ma, Z. Zhong, T.-M. Hsu, and F. Adib, "Learning food quality and safety from wireless stickers." in *HotNets*, 2018, pp. 106–112.